Supplementary Information

Mechanically-Sensitive Fluorochromism by Molecular Domino Transformation in a Schiff Base Crystal

Toshiyuki Sasaki,*[a] Takanori Nakane,[b] Akihiro Kawamoto,[b] Yakai Zhao,[c,d] Yushi Fujimoto,[e] Tomohiro Nishizawa,[f] Nabadeep Kalita,[g] Seiji Tsuzuki,*[h] Fuyuki Ito,*[e] Upadrasta Ramamurty,*[c,d] Ranjit Thakuria,*[g] Genji Kurisu*[b,i,j]

Affiliation

[a]*Japan Synchrotron Radiation Research Institute (JASRI), 1-1-1 Kouto, Sayo-cho, Sayo-gun, Hyogo 679-5198, Japan. E-mail: toshiyuki.sasaki@spring8.or.jp; t.devi.sasaki@gmail.com*

[b]*Institute for Protein Research, Osaka University, 3-2 Yamadaoka, Suita, Osaka 565-0871, Japan.*

[c]*School of Mechanical and Aerospace Engineering, Nanyang Technological University, Singapore 639798, Singapore. Email: satwiku@gmail.com*

[d]*Institute of Materials Research and Engineering, Agency for Science, Technology and Research (A*STAR), Singapore 138634, Singapore.*

[e]*Department of Chemistry, Institute of Education, Shinshu University, 6-ro, Nishinagano, Nagano, 380-8544, Japan. Email: fito@shinshu-u.ac.jp*

[f]*Department of Biological Sciences, Yokohama City University, 1-7-29 Suehiro-cho, Tsurumi-ku, Yokohama 230-0045, Japan.*

[g] *Department of Chemistry, Gauhati University, Guwahati 781014, Assam, India. Email: ranjit.thakuria@gmail.com, ranjit.thakuria@gauhati.ac.in*

[h] *Department of Applied Physics, The University of Tokyo, Hongo 7-3-1, Bunkyo-ku, Tokyo, 113-8656 Japan. E-mail: tsuzuki.seiji@mail.u-tokyo.ac.jp*

[i]*JEOL YOKOGUSHI Research Alliance Laboratories, Graduate School of Frontier Biosciences, Osaka University, 1-3 Yamadaoka, Suita, Osaka 565-0871 Japan.*

[j]*Institute for Open and Transdisciplinary Research Initiatives, Osaka University, 2-1 Yamadaoka, Suita, Osaka 565-0871, Japan. Email: gkurisu@protein.osaka-u.ac.jp*

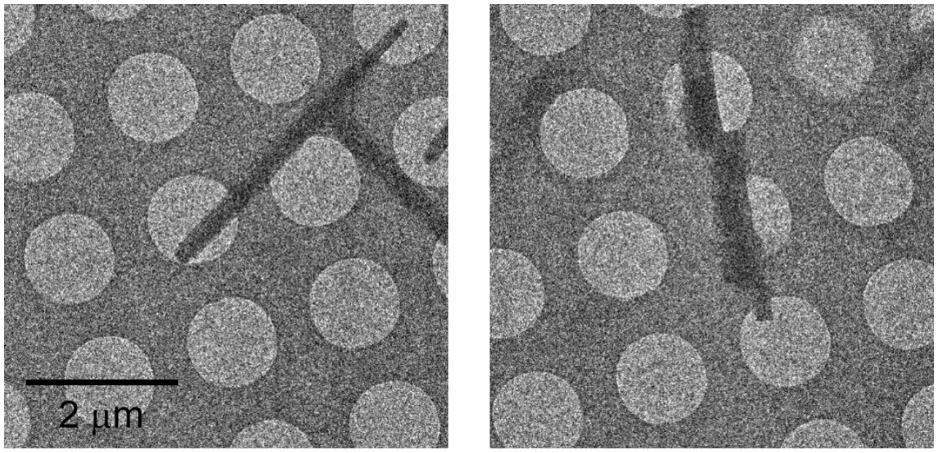

Fig. S1 Typical Cryo-EM images of 1. The crystal in the left panel was indexed in the orthorhombic crystal system (**1O**), while the crystal in the right panel was indexed in the monoclinic crystal system (**1Y**). Images of other crystals are deposited in XRDa.

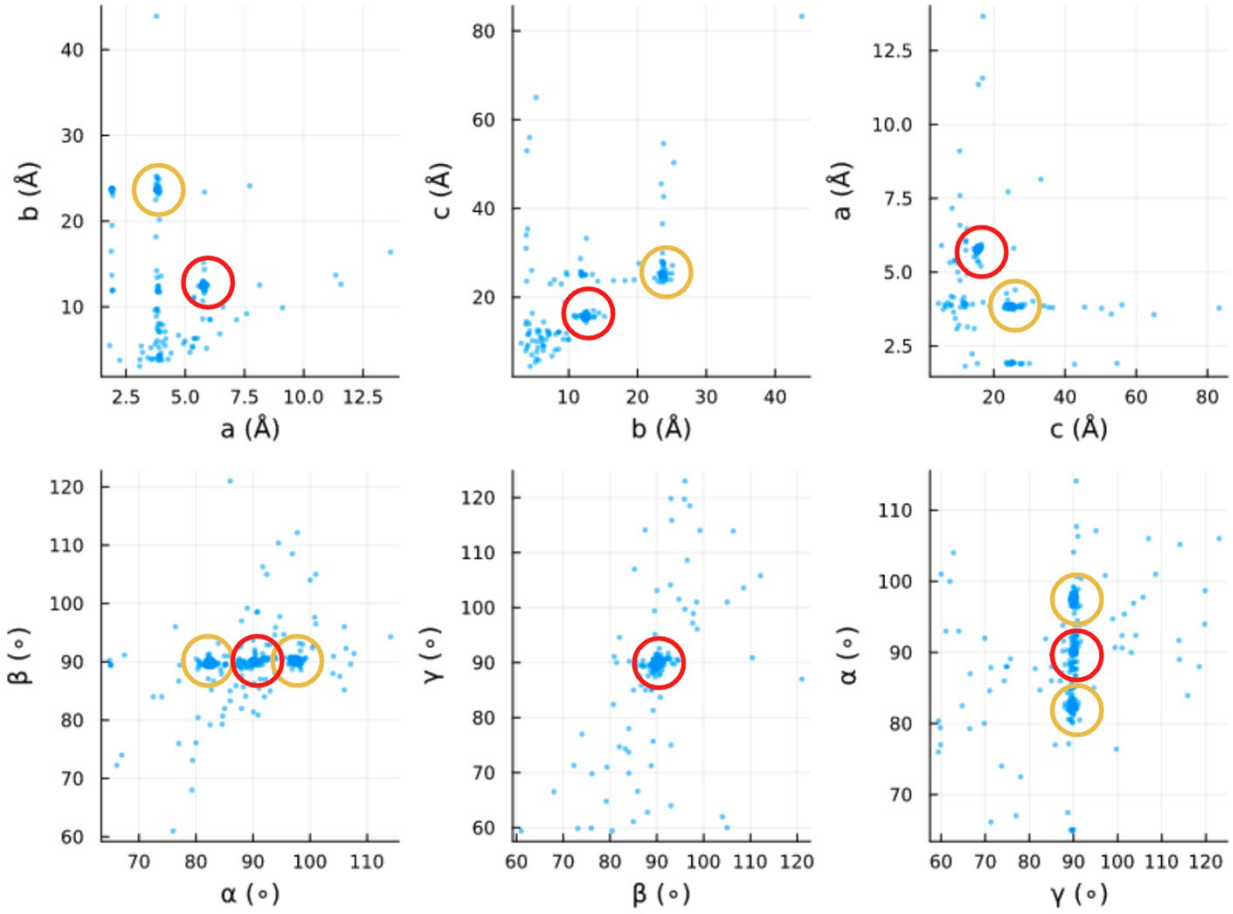

Fig. S2 Distribution of unit cell parameters from the first indexing trial. Note that Bravais lattice constraints were not applied and the diffraction geometry was not fully refined at this initial step of processing. Some dots correspond to mis-indexed, very weakly diffracting crystals. Monoclinic (**1Y**) and orthorhombic (**1O**) crystal forms are present and marked by orange and red circles, respectively. Monoclinic crystals are indexed in two settings (the β angle is split symmetrically around 90° to ~82° and ~98°).

Table S1 Merging statistics of 1O by MicroED.

d_max	d_min	#obs	#uniq	mult.	%comp	<I>	<I/sI>	r_mrg	r_means	r_pim	cc1/2
5.86	2.01	1050	164	6.40	84.54	2.9	20.1	0.089	0.096	0.034	0.996*
2.01	1.61	1901	196	9.7	100.00	1.4	12.5	0.164	0.172	0.048	0.996*
1.61	1.41	1469	170	8.64	100.00	0.6	5.1	0.235	0.248	0.076	0.983*
1.41	1.28	1154	151	7.64	100.00	0.4	3.0	0.289	0.308	0.100	0.970*
1.28	1.19	1909	181	10.55	100.00	0.5	3.6	0.269	0.282	0.080	0.995*
1.19	1.12	1814	177	10.25	100.00	0.5	4.1	0.237	0.248	0.069	0.991*
1.12	1.06	1673	164	10.2	100.00	0.3	2.7	0.334	0.349	0.096	0.976*
1.06	1.02	1466	156	9.4	100.00	0.3	2.3	0.32	0.337	0.099	0.974*
1.02	0.98	1365	150	9.1	100.00	0.2	1.3	0.504	0.533	0.162	0.936*
0.98	0.94	1416	153	9.25	100.00	0.2	1.0	0.553	0.582	0.170	0.919*
0.94	0.92	1975	177	11.16	100.00	0.1	0.6	0.982	1.022	0.271	0.636*
0.92	0.89	1842	166	11.1	100.00	0.1	0.8	0.894	0.933	0.253	0.737*
0.89	0.87	1691	165	10.25	100.00	0.1	0.6	0.972	1.013	0.271	0.491*
0.87	0.84	1685	162	10.4	100.00	0.0	0.5	1.324	1.381	0.372	0.470*
0.84	0.83	1659	158	10.5	100.00	0.0	0.4	1.513	1.576	0.419	0.385*
0.83	0.81	1592	152	10.47	100.00	0.0	0.4	1.987	2.069	0.553	0.157
0.81	0.79	1327	141	9.41	100.00	0.0	0.3	2.225	2.327	0.648	0.444*
0.79	0.78	1464	147	9.96	100.00	0.0	0.4	2.35	2.450	0.661	0.608*
0.78	0.76	1355	138	9.82	100.00	0.0	0.3	2.155	2.250	0.621	0.323*
0.76	0.75	1998	182	10.98	100.00	0.0	0.2	3.637	3.787	1.001	0.280*
5.86	0.75	31805	3250	9.79	99.72	0.4	3.2	0.296	0.311	0.089	0.995*

Table S2 Merging statistics of 1Y by MicroED.

d_max	d_min	#obs	#uniq	mult.	%comp	<I>	<I/sI>	r_mrg	r_means	r_pim	cc1/2
5.73	1.62	18417	312	59.03	96.89	8.3	38.0	0.151	0.152	0.020	0.996*
1.62	1.29	20831	289	72.08	98.30	3.0	24.9	0.198	0.199	0.022	0.990*
1.29	1.13	19005	278	68.36	98.58	3.0	20.9	0.199	0.201	0.024	0.990*
1.13	1.02	23324	292	79.88	98.32	2.5	21.0	0.21	0.212	0.023	0.966*
1.02	0.95	19247	270	71.29	98.54	1.2	10.9	0.318	0.320	0.036	0.993*
0.95	0.90	23405	295	79.34	98.33	1.0	9.8	0.339	0.341	0.037	0.970*
0.90	0.85	20491	270	75.89	98.18	0.7	7.2	0.439	0.442	0.049	0.964*
0.85	0.81	20343	273	74.52	98.56	0.5	5.0	0.562	0.567	0.064	0.889*
0.81	0.78	24240	288	84.17	98.63	0.5	5.3	0.529	0.532	0.056	0.982*
0.78	0.76	20951	275	76.19	97.86	0.3	3.5	0.72	0.726	0.080	0.879*
0.76	0.73	20493	266	77.04	98.15	0.3	3.0	0.777	0.783	0.086	0.849*
0.73	0.71	21569	280	77.03	98.94	0.2	2.3	0.918	0.925	0.103	0.810*
0.71	0.69	23230	280	82.96	98.25	0.2	2.4	0.921	0.927	0.099	0.805*
0.69	0.68	22843	280	81.58	98.94	0.2	2.0	1.12	1.128	0.122	0.823*
0.68	0.66	20625	262	78.72	98.50	0.2	1.8	1.291	1.300	0.141	0.834*
0.66	0.65	20223	273	74.08	98.56	0.1	1.1	1.67	1.683	0.190	0.603*
0.65	0.63	22338	284	78.65	98.95	0.1	1.1	1.777	1.790	0.195	0.800*
0.63	0.62	21517	258	83.40	98.47	0.1	0.9	2.174	2.190	0.234	0.260*
0.62	0.61	23945	289	82.85	98.97	0.1	0.9	2.262	2.278	0.242	0.326*
0.61	0.60	21309	266	80.11	98.52	0.1	0.7	2.794	2.814	0.302	0.244*
5.73	0.6	428346	5580	76.76	98.41	1.2	8.4	0.327	0.330	0.037	0.995*

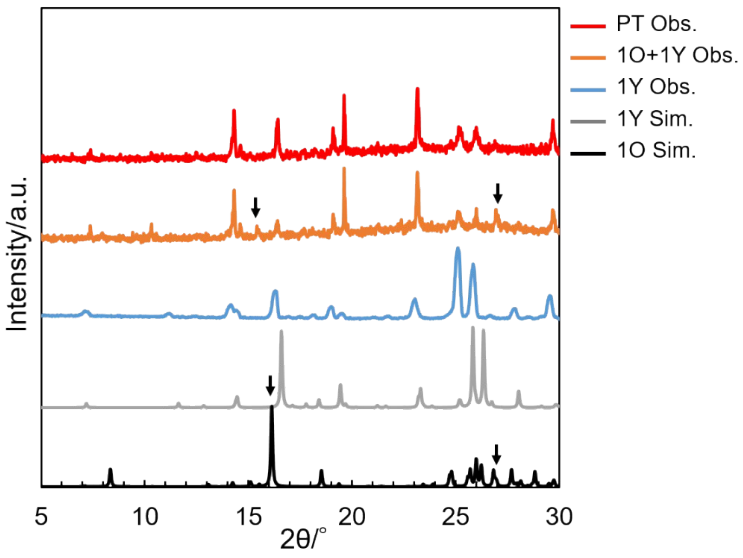

Fig. S3 Powder X-ray diffraction (PXRD) patterns of 1O and 1Y. Black and gray lines represent simulated PXRD of **1O** (1O Sim.) and **1Y** (1Y Sim.) from the crystal structure solved by MicroED. Experimentally obtained PXRD patterns of **1Y** (1Y Obs.), a mixture of **1O** and **1Y** (1O+1Y Obs.), and the mixture after phase transformation from **1O** into **1Y** (PT Obs.) are drawn by blue, orange, and red solid lines, respectively. Representative peaks from **1O** are indicated by black arrows.

Table S3 Crystallographic parameters of 1O and 1Y solved by MicroED (λ = 0.02508 Å).

Polymorphs	**1O**	**1Y**
Chemical formula	C13 H10 N2 O3	C13 H10 N2 O3
Formula wt	242.23	242.23
Cryst syst	Orthorhombic	Monoclinic
Space group	$Pna2_1$	$P2_1/c$
T, K	79	79
a, Å	23.456	12.450
b, Å	3.811	5.735
c, Å	24.879	15.344
α, deg	90	90
β, deg	90	97.73
γ, deg	90	90
Z	8	4
V, Å^3	2224.2	1085.6
D_{calc}, g cm^{-3}	1.447	1.482
reflns collected	21049	208643
unique reflns	3836	2657
R1[I > 2(I)]	0.1215	0.1774
wR2 (all)	0.3097	0.4522
GOF	0.864	1.253
Data collection	Talos Arctica microscope	Talos Arctica microscope
High resolution limit for refinement, Å	0.84	0.75
COD ID.	3000450	3000451
CCDC no.	2279131	2279132

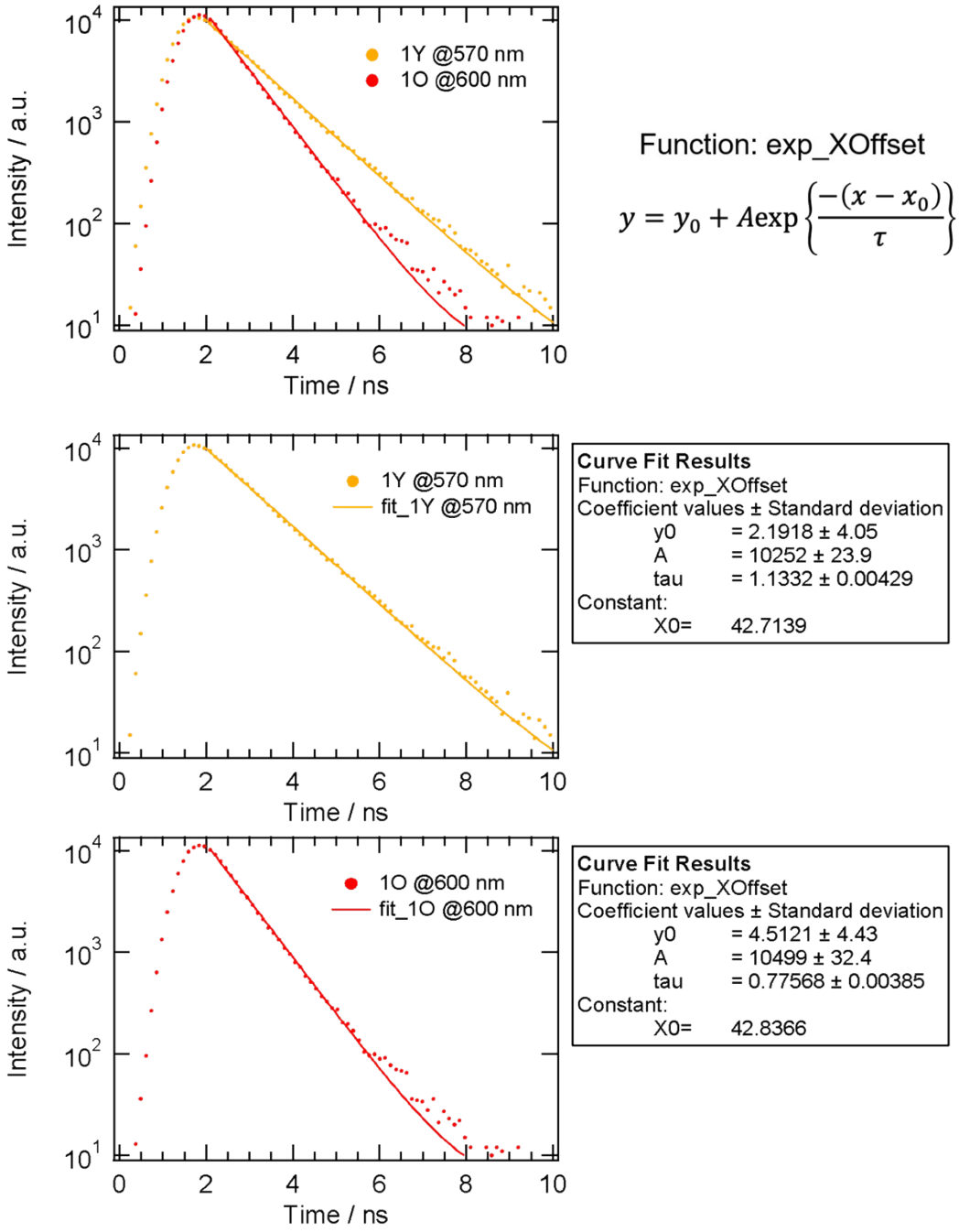

Fig. S4 Fluorescence lifetimes. The lifetimes were measured from a single crystal by a unit consisted of a pico pulse laser (375 nm, 50 MHz) (LDB 160C, Tama Electric Inc.), an avalanche photodiode detector (MPD, Becker & Hickl GmbH), and a counting board (SPC-130, Becker & Hickl GmbH). Filters: a sharp-cut filter (L42, HOYA), and optical bandpass filters (570 nm or 600 nm, 10 nm bandwidth in fwhm), were used to select the monitoring wavelength and avoid the scattering excitation light. **1Y** and **1O** crystals for the measurements were selected based on their emission colors under UV light.

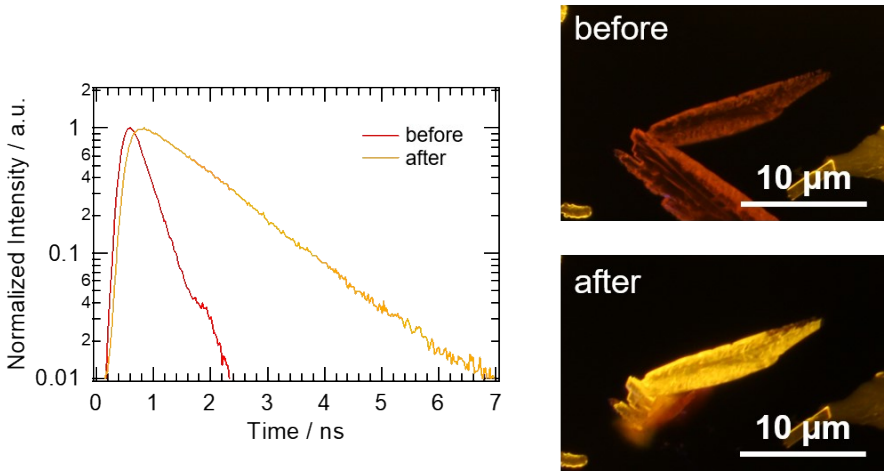

Fig. S5 Change of fluorescence lifetime by MDT. Fluorescence lifetimes of **1O** before (before, red solid line) and after (after, yellow solid line) MDT which was induced by a mechanical stimulus.

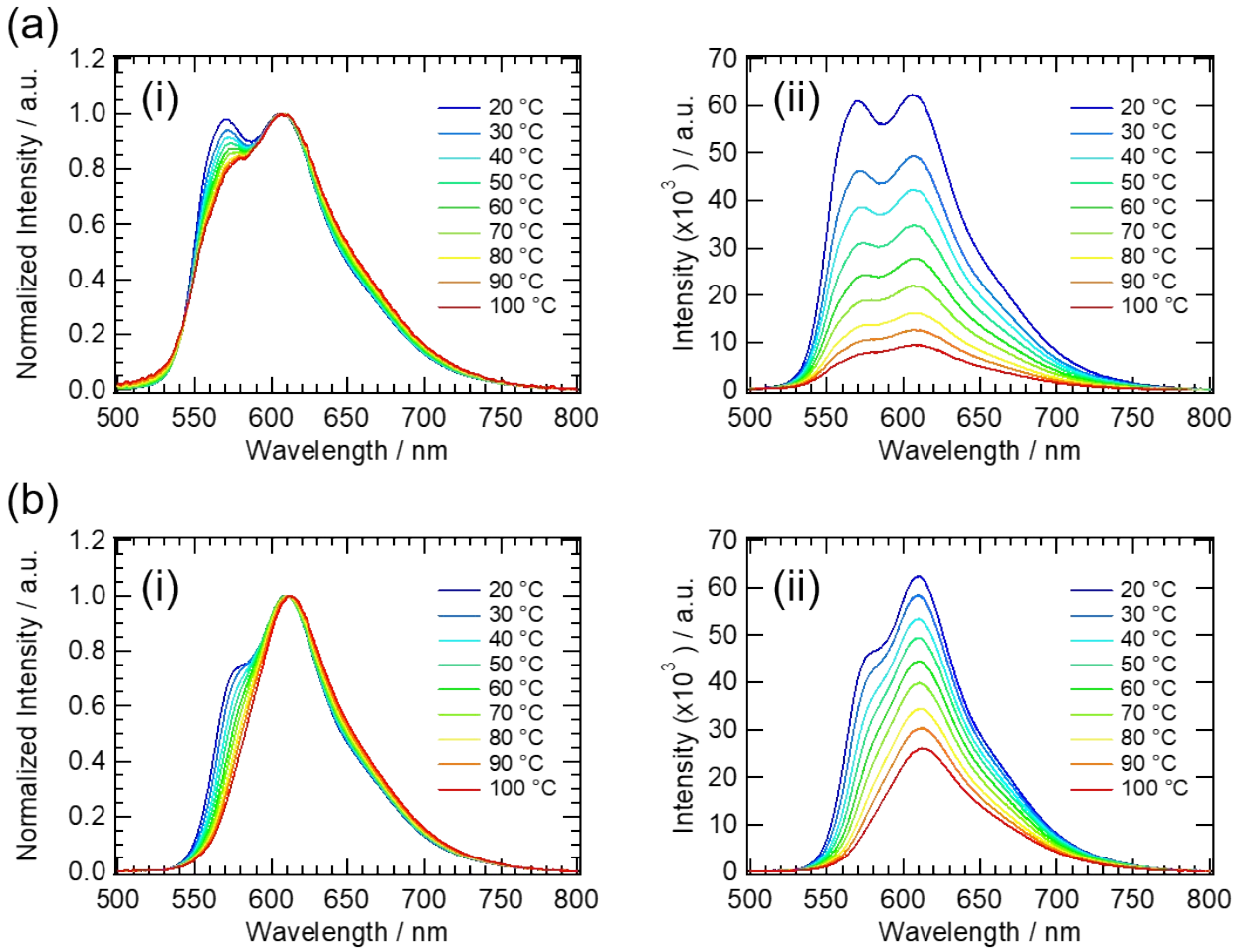

Fig. S6 Temeperature-dependent emission. Temperature-dependent fluorescent spectra of (a) **1Y** and (b) **1O** from 20 °C to 100 °C.

Table S4 Calculated lattice energies of 1O and 1Y.[a]

	1O	1Y
Lattice energy	228.3 (28.5)	116.4 (29.1)[a]

[a] Energy in kcal/mol. **1O** has eight molecules in one unit cell, while **1Y** has four molecules in one unit cell. The lattice energy per molecule is shown in parenthesis.

Lattice energy calculation

The lattice energy ($E_{lattice}$) was calculated using Quantum ESPRESSO program with the PBE functional [67] and Grimme's D3BJ dispersion correction. [68] The self-consistent calculations are computed with the cutoff energy of 36 Ry for the plane wave and 324 Ry for electron densities, respectively. The $E_{lattice}$ was obtained according to the equation using optimized geometries,

$$E_{lattice} = -(E_{cryst} - n\,E_{mono}).$$

where E_{cryst} is the energy of the unit cell of crystal calculated using the periodic boundary condition, E_{mono} is the energy of the isolated molecule, and n is the number of molecules in one unit cell. The position of atoms in crystals were optimized, while the cell parameters were fixed at experimental values in the optimizations. The geometry of isolated molecule was optimized. The molecule was isolated by the cubic unit cell with the edge of 25 Å in the calculations of E_{mono}. The geometries of monomers obtained by the optimizations of position of atoms in crystals are shown in Fig. S6a-c. The torsional angles in the optimized geometries are summarized in Table S5.

Table S5 Torsional angles of optimized molecules in crystals[a]

	2-1-7-8	3-4-10-11	4-10-11-12	10-11-12-13
1Y	-7.7	-6.7	177.9	3.3
1O (i)	-4.9	32.4	-175.9	-0.9
1O (ii)	-6.1	-35.4	173.9	-0.6

[a] Torsional angle in degree.

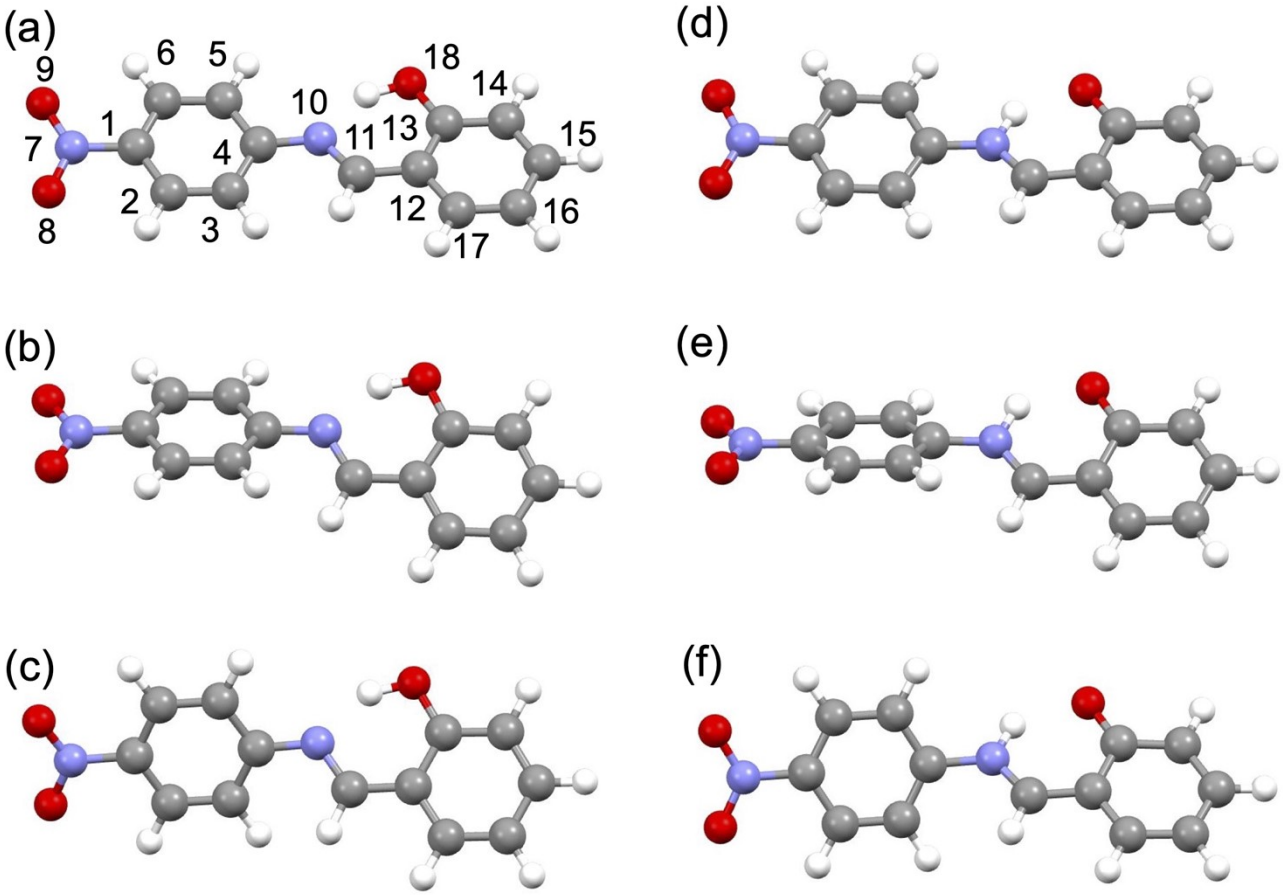

Figure S7. Optimized structures of **1** in ground states and excited states: (a) ground state structure in crystal **1Y**; (b) ground state structure in crystal in **1O (i)**; (c) ground state structure in crystal in **1O (ii)**; (d) excited state structure in crystal **1Y**; (e) excited state structure in crystal **1O (i)**; (f) excited state structure in crystal **1O (ii)**

Table S6 Wavelengths of three longest fluorescence spectra and their oscillator strength (f) calculated for 1O and 1Y.

1O[a]	**1Y**
688 nm (f=0.1119) / 672 nm (f=0.1245)	617 nm (f=0.1765)
468 nm (f=0.0054) / 466 nm (f=0.0041)	462 nm (f=0.0005)
428 nm (f=0.0924) / 428 nm (f=0.0835)	4254 nm (f=0.0402)

[a] Calculated for two crystallographically independent molecules.

Calculations of fluorescence spectra

The Gaussian 16 program was used for the calculations. The optimizations of excited state geometries of isolated molecules and the calculations of their fluorescence spectra were carried out using the time-dependent DFT method. [69] The B3LYP functional [70] and 6-311G** basis set were used for the calculations. The optimized ground state

geometries in the crystals (Figs. S7a-c) were used for initial geometries of the optimizations of excited state geometries. The torsional angles of four rotatable bonds shown in Table S5 were fixed in the geometry optimizations in the excited state. The optimized geometries of isolated molecules in excited states are shown in Fig. S7d-f.

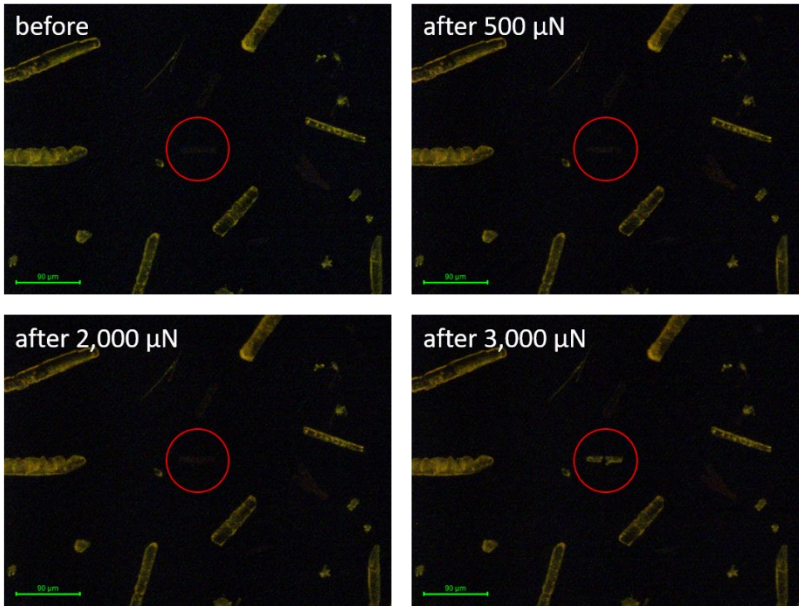

Fig. S8 Photographic images **1** under UV light before and after nanoindentation (Hysitron TI980, Bruker Corp.) with a foce of 500 μN, 2,000 μN, and 3,000 μN. Mechanically stimulated **1O** is circled by red. Nanoindentation always started the identation tests from very low load (~ 1 μN) and then conducted tests with progressively higher loads until MDT happened.

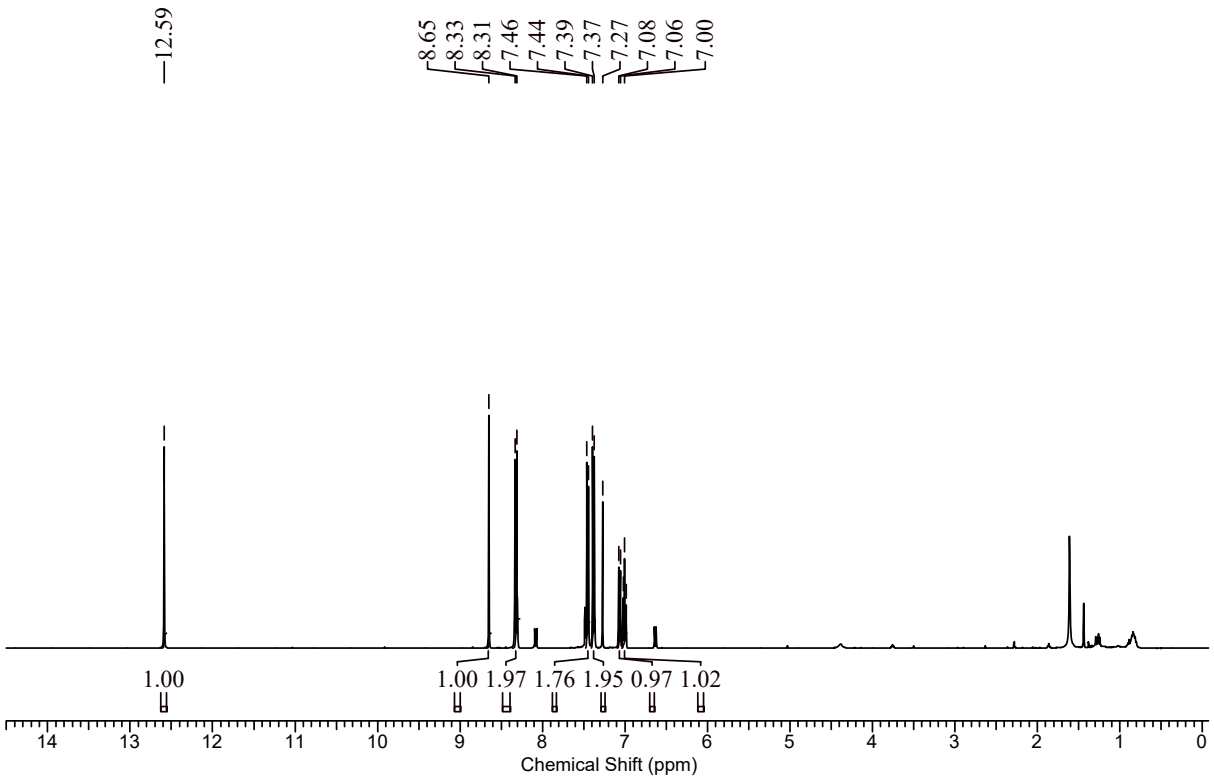

Fig. S9 ^{1}H NMR: 12.59 (s, 1H), 8.65 (s, 1H), 8.32 (d, J= 8 Hz, 2H), 7.45 (d, J=8 Hz, 2H), 7.38 (d, J=8 Hz, 2H), 7.07 (d, J=8 Hz, 1H), 7.00 (t, J=8 Hz, 1H).

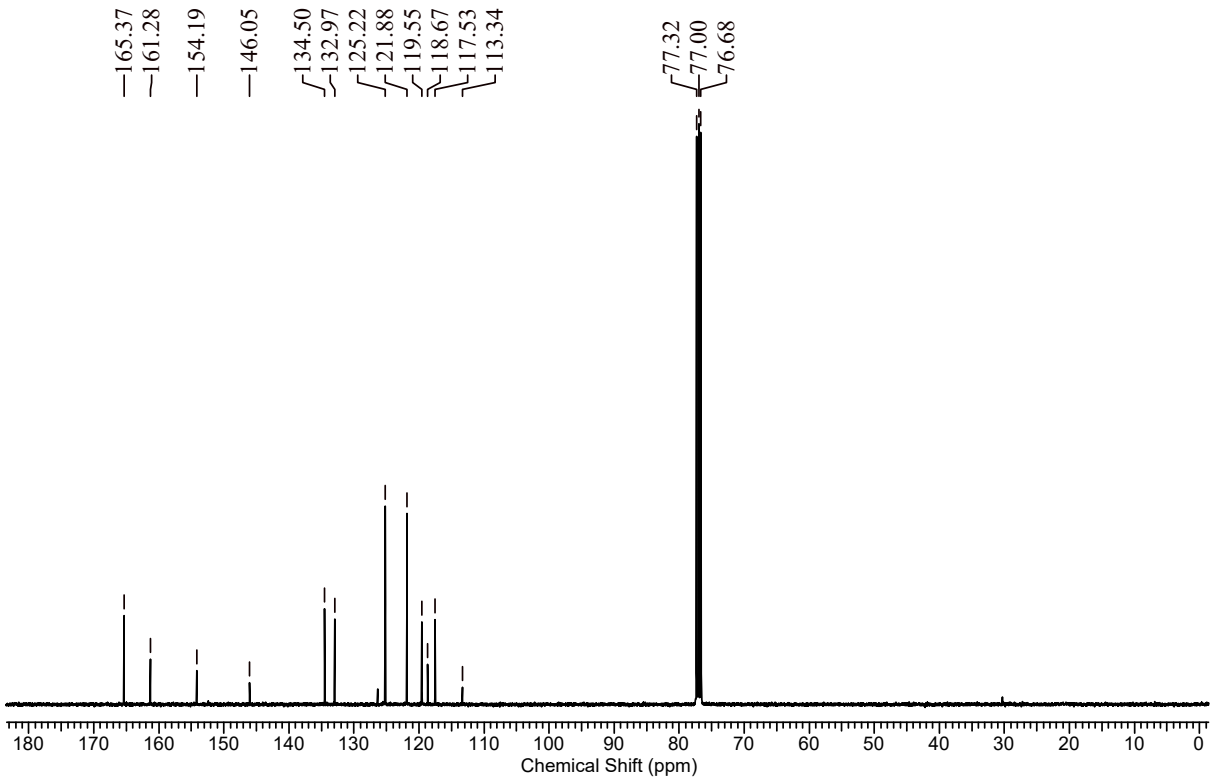

Fig. S10 ^{13}C NMR: 165.3, 161.2, 154.1, 146.0, 134.5, 132.9, 125.2, 121.8, 119.5, 118.6, 117.5 and 113.3.

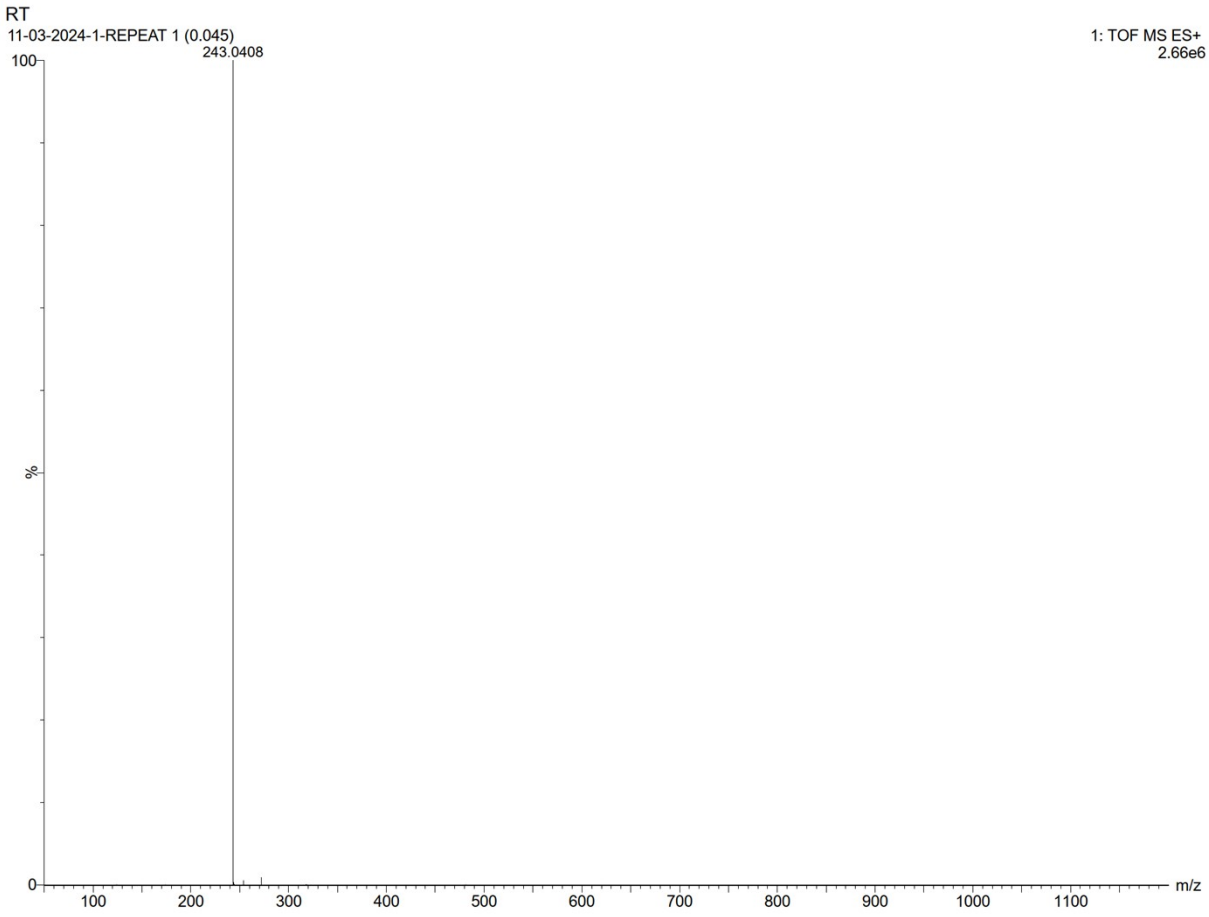

Fig. S11 HR-MS spectrum of **1**. Mass calculated for $C_{13}H_{10}N_2O_3$ as $[M+H]^+$ is 243.0764 and obtained mass is 243.0408 (100%). From this data, the synthesized compound **1** can be considered to be in the pure form.

References

[67] J. P. Perdew, K. Burke and M. Ernzerhof, *Phys. Rev. Lett.* 1996, **77***,* 3865–3868.

[68] S. Grimme, S. Ehrlich and L. Goerigk, *J. Comp. Chem*. 2011, **32**, 1456–1465.

[69] R. Bauernschmitt and R. Ahlrichs, *Chem. Phys. Lett.* 1996, **256**, 454–464.

[70] A. D. Becke, *J. Chem. Phys.* 1993, **98**, 5648–5652.